

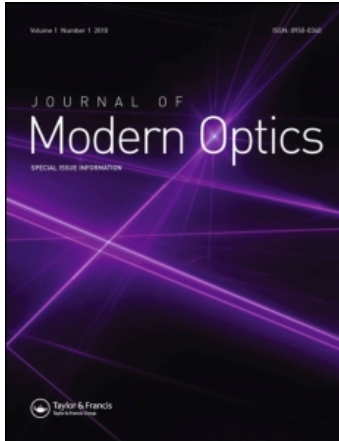
This article was downloaded by: [MPI Max-Planck-Institute Fuer Quantenoptik]

On: 29 July 2010

Access details: Access Details: [subscription number 918253081]

Publisher Taylor & Francis

Informa Ltd Registered in England and Wales Registered Number: 1072954 Registered office: Mortimer House, 37-41 Mortimer Street, London W1T 3JH, UK



## Journal of Modern Optics

Publication details, including instructions for authors and subscription information:

<http://www.informaworld.com/smpp/title~content=t713191304>

### Non-sequential double ionization in a few-cycle laser pulse: the influence of the carrier-envelope phase

H. Rottke<sup>a</sup>; X. Liu<sup>ab</sup>; E. Eremina<sup>a</sup>; W. Sandner<sup>a</sup>; E. Goulielmakis<sup>cd</sup>; K. O. Keeffe<sup>d</sup>; M. Lezius<sup>d</sup>; F. Krausz<sup>cd</sup>; F. Lindner<sup>c</sup>; M. G. SchÄtzel<sup>c</sup>; G. G. Paulus<sup>be</sup>; H. Walther<sup>ce</sup>

<sup>a</sup> Max-Born-Institut, D-12489 Berlin, Germany <sup>b</sup> Texas A&M University, Dept. of Physics, College Station, TX 77843-4242, USA <sup>c</sup> Max-Planck-Institut für Quantenoptik, D-85748 Garching, Germany <sup>d</sup> Institut für Photonik, Technische Universität Wien, A-1040 Wien, Austria <sup>e</sup> Ludwig-Maximilians-Universität München, D-85748 Garching, Germany

**To cite this Article** Rottke, H. , Liu, X. , Eremina, E. , Sandner, W. , Goulielmakis, E. , Keeffe, K. O. , Lezius, M. , Krausz, F. , Lindner, F. , SchÄtzel, M. G. , Paulus, G. G. and Walther, H.(2006) 'Non-sequential double ionization in a few-cycle laser pulse: the influence of the carrier-envelope phase', Journal of Modern Optics, 53: 1, 149 – 162

**To link to this Article:** DOI: 10.1080/09500340500186107

**URL:** <http://dx.doi.org/10.1080/09500340500186107>

## PLEASE SCROLL DOWN FOR ARTICLE

Full terms and conditions of use: <http://www.informaworld.com/terms-and-conditions-of-access.pdf>

This article may be used for research, teaching and private study purposes. Any substantial or systematic reproduction, re-distribution, re-selling, loan or sub-licensing, systematic supply or distribution in any form to anyone is expressly forbidden.

The publisher does not give any warranty express or implied or make any representation that the contents will be complete or accurate or up to date. The accuracy of any instructions, formulae and drug doses should be independently verified with primary sources. The publisher shall not be liable for any loss, actions, claims, proceedings, demand or costs or damages whatsoever or howsoever caused arising directly or indirectly in connection with or arising out of the use of this material.

## Non-sequential double ionization in a few-cycle laser pulse: the influence of the carrier–envelope phase

H. ROTTKE\*<sup>†</sup>, X. LIU<sup>‡</sup>, E. EREMINA<sup>†</sup>, W. SANDNER<sup>†</sup>,  
E. GOULIELMAKIS<sup>¶</sup>, K. O. KEEFFE<sup>¶</sup>, M. LEZIUS<sup>¶</sup>, F. KRAUSZ<sup>¶</sup>,  
F. LINDNER<sup>§</sup>, M. G. SCHÄTZEL<sup>§</sup>, G. G. PAULUS<sup>‡</sup> and H. WALTHER<sup>||</sup>

<sup>†</sup>Max-Born-Institut, Max-Born-Str. 2a, D-12489 Berlin, Germany

<sup>‡</sup>Texas A&M University, Dept. of Physics, College Station, TX 77843-4242, USA

<sup>§</sup>Max-Planck-Institut für Quantenoptik, Hans-Kopfermann-Str. 1,  
D-85748 Garching, Germany

<sup>¶</sup>Institut für Photonik, Technische Universität Wien, Gusshausstr. 27,  
A-1040 Wien, Austria

<sup>||</sup>Ludwig-Maximilians-Universität München, Am Coulombwall 1,  
D-85748 Garching, Germany

(Received 18 March 2005)

Non-sequential double ionization (NSDI) using phase-stabilised few-cycle laser pulses is investigated. We report differential measurements of  $\text{Ar}^{++}$  ion momentum distributions. They show a strong dependence on the carrier-envelope (CE) phase. Via control over the CE phase one is able to direct the NSDI dynamics. Data analysis through a classical model calculation reveals that the influence of the optical phase enters via: (1) the cycle-dependent electric field ionization rate, (2) the electron recollision time and (3) the accessible phase space for inelastic collisions. Our model indicates that the combination of these effects allows a look into single-cycle dynamics already for few-cycle pulses.

### 1. Introduction

Recent advances in femtosecond laser technology have opened the door to unprecedented insight into intense laser–matter interaction (up to 100 GW) on the time-scale of a few optical cycles [1]. The time evolution of the electric field strength,  $E(t) = E_0(t) \cos(\omega t + \varphi)$ , of these few-cycle pulses depends strongly on the phase  $\varphi$  that the carrier wave  $\cos(\omega t + \varphi)$  has relative to the pulse envelope  $E_0(t)$ , the so-called carrier-envelope (CE) phase [2]. Since the pioneering work of [3] feedback control of the CE phase has been established [4] and a direct measurement of  $\varphi$  was demonstrated recently [5, 6]. Today, besides being precisely known the spatio-temporal variation of electromagnetic fields consisting of a few cycles can be shaped with attosecond precision via control of the CE phase  $\varphi$ .

---

\*Corresponding author. Email: rottke@mbi-berlin.de

Double ionization of atoms at high light intensity in ultra-short laser pulses has been found to proceed non-sequentially as long as the probability to singly ionize the atom stays low. This first became evident in unusually high double ionization rates [7–11]. A first hint to the mechanism behind non-sequential double ionization (NSDI) came from the dependence of the total yield of doubly charged ions on the ellipticity of the light beam polarization [10, 12]. These experiments indicated that inelastically scattered electrons that were driven back to the ion core by the oscillating laser field may be responsible for NSDI. This mechanism has been further confirmed through measuring the momentum distributions of doubly charged He and Ne ions [13, 14], in kinematically complete momentum spectroscopy on the final state photoelectrons and on the ion [15–22], and in electron kinetic energy distributions measured in coincidence with doubly charged ions [23–26]. The same electron scattering mechanism [27] has been found to be responsible for the generation of high-order harmonics of a laser pulse [28] and for high-energy photoelectrons emerging from single ionization [29].

In the quasistatic limit NSDI can be viewed to be initiated by electric field ionization of one electron. Being in the continuum the further motion of this electron is mainly governed by the electric field of the light wave. Under specific initial conditions the electron returns back to the singly charged ion core and collides. A classical analysis of the motion shows that the maximum kinetic energy,  $E_{\text{kin,max}}$ , the returning electron can have is  $3.17 U_p$ , where  $U_p$  denotes the ponderomotive energy.  $U_p$  measures the quiver energy of a free electron in an oscillating electric field. It is proportional to the laser intensity. Depending on  $E_{\text{kin,max}}$  different routes to double ionization are possible: (1) instantaneous *impact ionization* of the singly charged ion, or (2) *impact excitation* of the ion core with subsequent electric field ionization of the excited ion [16, 30, 31]. NSDI causes dislodging of two electrons from the ion core. It thus represents an excellent example for a heavily perturbed three-body Coulomb system.

Control of the CE phase  $\varphi$  of a few-cycle light pulse and the exponential dependence of the atomic electric field (tunnel) ionization rate on the instantaneous electric field strength have opened the opportunity to define the moment of ionization of an atom to within several hundred attoseconds [32, 33]. The trajectory of the photoelectron born within this narrow time window remains subject to the laser field, which can—in principle—be tailored at will. This allows for control over the various recollision processes of the field-liberated electron. Indeed, it has been found that for high harmonic generation (HHG) [5] and high-order above threshold ionization (ATI) [6] the experimentally observed outcomes are strongly dependent on  $\varphi$ . Similar to HHG and ATI, also for NSDI a significant sensitivity on  $\varphi$  has been predicted for the final state electron–electron momentum correlation [34] and has been observed for the recoil ion momentum distribution [35]. This indicates the possibility to steer atomic double ionization efficiently using the CE phase  $\varphi$ .

We will start outlining the simple classical model which serves to simulate the main features of the strong field double ionization dynamics in a few-cycle laser pulse. Next, the experimental set-up we used to investigate few-cycle NSDI will be presented. To allow the realization of the experiment, state-of-the-art sophisticated techniques from different fields had to be brought together: a laser system delivering

few-cycle pulses with the CE phase stabilized, a means to monitor the CE phase and compensate for long term drift of the phase, and a set-up which allows the measurement of the sum-momentum distribution of the electrons emitted in NSDI. The electron sum-momentum is determined by measuring the equivalent momentum of the corresponding doubly charged ion using ‘cold target recoil ion momentum spectroscopy’ (COLTRIMS) [36]. Our model results are compared with experimentally observed ion momentum distributions using argon. Qualitatively, they are able to explain the observed dependence of the  $\text{Ar}^{++}$  ion momentum distributions on the CE phase. Moreover, the model indicates that we are able to look into single-cycle dynamics of NSDI even though the light pulses used in the experiment still consist of several optical cycles.

## 2. Theoretical model for NSDI

In the model a few-cycle laser pulse is characterized via its vector potential  $\mathbf{A}(t)$ . We use a specific simple pulse form in the calculations:

$$\mathbf{A}(t) = \begin{cases} \mathbf{A}_0 \cos^2[\omega t/(2N)] \sin(\omega t + \varphi), & t \in [-NT/2, NT/2], \\ 0, & \text{otherwise.} \end{cases} \quad (1)$$

$N$  is the number of cycles in the pulse,  $\omega$  is its carrier frequency and  $T = 2\pi/\omega$  is the carrier oscillation period. Starting from the vector potential the electric field of the light pulse is given by  $\mathbf{E}(t) = -d\mathbf{A}(t)/dt$ . This way to determine the electric field strength fixes the pulse area to zero ( $\int_{-\infty}^{\infty} dt \mathbf{E}(t) = 0$ ), independent of the setting of the CE phase  $\varphi$ . A laser pulse requires a zero pulse area for the electric field. Otherwise, its spectrum would contain an unphysical DC component. A zero pulse area at any setting of  $\varphi$  would not have been achieved by simply putting a pulse envelope function  $\mathbf{E}_0 \cos^2[\omega t/(2N)]$  into the simplified definition of the electric field strength given in section 1.

Down to  $N = 3$  optical cycles the envelope function of  $|\mathbf{E}(t)|^2$  for the pulse defined above is very well given by  $|\mathbf{E}_0|^2 \cos^4[\omega t/(2N)]$  (with  $\mathbf{A}_0 = \mathbf{E}_0/\omega$ ). For a large number  $N$  of cycles this envelope function is proportional to the light intensity at time  $t$  in the pulse. Using the envelope a width (full width at half maximum, FWHM) can roughly be assigned to the pulse given above to be  $FWHM \approx 0.36NT$ . This definition has a limited meaning in the few-cycle regime since the detailed dependence of the pulse on time depends sensitively on the CE phase. As an example, the electric field strength is shown for an  $N = 4$  cycle pulse in the upper panel of figure 1 for several settings of the CE phase ((a)  $\varphi = -0.3\pi$ , (b)  $\varphi = 0.15\pi$  and (c)  $\varphi = 0.7\pi$ ).

The simplified laser pulse defined above is plugged into the classical model to simulate NSDI. It is closely related to the quantum mechanical strong field S-matrix theory with only impact ionization caused by the recolliding electron taken into account. In the classically accessible phase space the final state electron momentum correlation calculated with the classical approach is in close agreement with the corresponding quantum mechanical S-matrix result, provided the collision energy  $E_{\text{kin,max}}$  of the returning electron is large enough compared to the ionization potential  $I_p^+$  of the singly charged ion core [38]. In the adjacent, classically

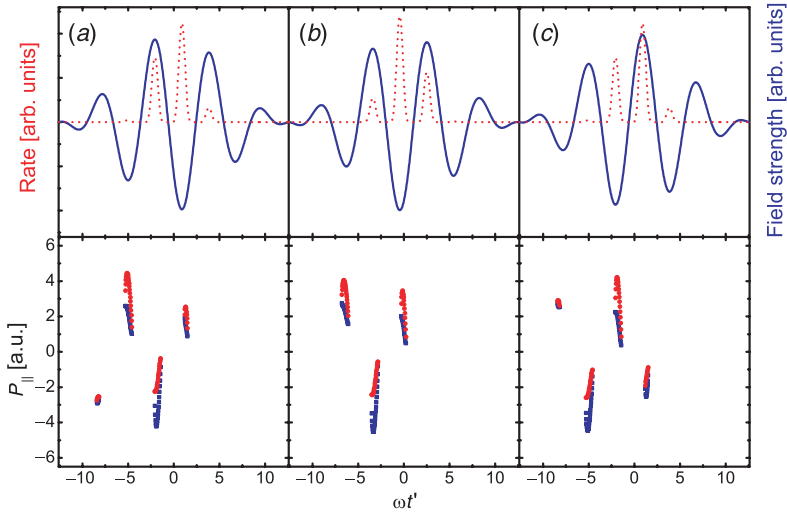


Figure 1. Upper panel: electric field  $E(t)$  (solid line) and the quasistatic field ionization rate [37] (dotted line) of Ar for a 4-cycle laser pulse (light peak intensity:  $350 \text{ TW cm}^{-2}$ ) at several CE phase settings: (a)  $\varphi = -0.3\pi$ , (b)  $\varphi = 0.15\pi$  and (c)  $\varphi = 0.7\pi$ . Lower panel: the corresponding classically accessible final state phase space for the sum-momentum  $P_{\parallel}$  of the two free electrons with the recolliding electron liberated at time  $t'$  in units of the optical period (upper boundary (dots) and lower one (squares)). The transverse momenta of the two electrons are assumed to be zero ( $\mathbf{p}_{\perp} = \mathbf{p}_{2\perp} = 0$ ). (The colour version of this figure is included in the online version of the journal.)

inaccessible, final state phase space, the quantum mechanical S-matrix decays to zero exponentially fast.

The final state classical differential two-electron momentum distribution  $\Gamma_{\varphi}(\mathbf{p}_1, \mathbf{p}_2)$  can be written in the form [38]:

$$\Gamma_{\varphi}(\mathbf{p}_1, \mathbf{p}_2) \propto \int_{-\infty}^{\infty} dt' R(t') \delta \left( E_{\text{kin}}(t'') - \sum_{i=1}^2 \frac{1}{2} [\mathbf{p}_i + \mathbf{A}(t'')]^2 - I_p^+ \right) |V_{\mathbf{p}_1, \mathbf{p}_2, \mathbf{k}}|^2. \quad (2)$$

At time  $t'$  the electron, which later on recollides with the ion core, appears in the ionization continuum through electric field ionization with an instantaneous ionization rate  $R(t')$ . We use the Keldysh expression for the rate [39]:

$$R(t') \propto \frac{1}{|\mathbf{E}(t')|} \exp \left[ -\frac{2(2I_p)^{3/2}}{3|\mathbf{E}(t')|} \right], \quad (3)$$

where  $I_p$  is the ionization potential of the atom and  $\mathbf{E}(t')$  is the electric field strength in the laser pulse at time  $t'$ . After the electron has entered the ionization continuum we assume that the external electric field alone determines its motion. At time  $t'$  we assume as initial condition for this motion that the electron is at rest. This fixes the intermediate state momentum  $\mathbf{k}$ :

$$\mathbf{k} + \mathbf{A}(t') = 0. \quad (4)$$

Non-sequential double ionization necessitates that the electron returns back to the singly charged ion core at some time  $t'' > t'$ . The return condition can be expressed as

$$\int_{t'}^{t''} dt [\mathbf{k} + \mathbf{A}(t)] = 0. \quad (5)$$

This fixes  $t''$  in equation (2). At this time we assume the electron collides inelastically with a second electron which is still bound to the ion core. The kinetic energy of the electron when it collides is given by

$$E_{\text{kin}}(t'') = \frac{1}{2} [\mathbf{k} + \mathbf{A}(t'')]^2.$$

Depending on  $t'$  equation (5) may have several solutions  $t''$ . In our simple model we take into account only the first encounter with the ion core, i.e. the time  $t''$  closest to  $t'$ . Due to the longer travel time later returns are expected to contribute significantly less to the integral in equation (2) since the quantum mechanical electron wave packet increasingly spreads with time.

The inelastic collision at  $t''$  is taken into account in equation (2) through the quantum mechanical transition matrix element  $V_{\mathbf{p}_1, \mathbf{p}_2, \mathbf{k}}$ . It is treated in first-order Born approximation. In the initial state the colliding electron is in a plane wave intermediate Volkov state [38]  $|\mathbf{k} + \mathbf{A}(t'')\rangle$  and the electron which is bound to the ion core in a state  $\phi^{(2)}$ . After the collision both electrons are in the continuum in Volkov states  $|\mathbf{p}_i + \mathbf{A}(t'')\rangle$  ( $i = 1, 2$ ):

$$V_{\mathbf{p}_1, \mathbf{p}_2, \mathbf{k}} = \langle \mathbf{p}_1 + \mathbf{A}(t''), \mathbf{p}_2 + \mathbf{A}(t'') | V(\mathbf{x}_1, \mathbf{x}_2) | \mathbf{k} + \mathbf{A}(t''), \phi^{(2)} \rangle. \quad (6)$$

This matrix element and therefore equation (2) is gauge dependent via the Volkov states. We use the length gauge in the model calculation. The electron–electron interaction  $V(\mathbf{x}_1, \mathbf{x}_2)$  is assumed to be a contact interaction. In addition, we assume that the collision is only allowed to happen at the point where the ion core is located. We then get  $V_{\mathbf{p}_1, \mathbf{p}_2, \mathbf{k}} = V_0 \phi^{(2)}(0)$ , i.e. a constant.  $V_0$  is the strength of the contact interaction. For ‘long’ laser pulses ( $N \approx 30$ ) this very crude choice of interaction is known to give rise to an electron momentum correlation for the momentum components parallel to the electric field of the light pulse which qualitatively closely agrees with the experimental results, provided the main ionization mechanism in the recollision event is impact ionization and  $E_{\text{kin}, \text{max}}(t'') \gg I_p^+$ .

The  $\delta$ -function under the integral in equation (2) serves to take care of energy conservation in the inelastic electron–electron collision. The excess energy which can be distributed among the two free final state electrons is  $E_{\text{kin}}(t'') - I_p^+$  with  $E_{\text{kin}}(t'')$  the kinetic energy of the recolliding electron and  $I_p^+$  the ionization potential of the singly charged ion.

In figure 1 besides the electric field, the instantaneous electric field ionization rate  $R(t')$  (equation (3)) is plotted for the 4-cycle pulses with different CE phase (upper panel, dashed lines). The light intensity was assumed to be  $350 \text{ TW cm}^{-2}$  and the ionization potential  $I_p$  of Ar was used to calculate  $R(t')$ . Only three half-cycles provide significant bursts of free electrons through field ionization and thus initiate NSDI. The full widths at half maximum of these bursts is  $\text{FWHM} \approx 0.13T$ .

For typical few-cycle Ti:sapphire laser pulses at a centre wavelength of 760 nm this amounts to a FWHM  $\approx 350$  as.

The lower panel in figure 1 visualizes the classically accessible final state phase space for the sum-momentum  $P_{\parallel}$  of the two free electrons after impact ionization as a function of the release time  $t'$  of the recolliding electron. The second ionization potential  $I_p^+$  of Ar was used for the calculation. Shown is the upper (dots) and lower (squares) boundary of the phase space assuming that  $\mathbf{p}_{1,\perp} = \mathbf{p}_{2,\perp} = 0$  with  $\mathbf{p}_{i,\perp}$  the momentum components of the electrons perpendicular to the electric field of the light pulse. Depending on the half-cycle, the sign of the sum-momentum of the electrons is either positive ( $P_{\parallel} > 0$ ) or negative ( $P_{\parallel} < 0$ ) for every setting of the CE phase (figure 1). For every  $\varphi$  three major phase space islands are accessible in three successive half-cycles. In all other half-cycles the kinetic energy of the colliding electron is smaller than the ionization potential  $I_p^+$  of the singly charged ion. In this case impact ionization is classically forbidden.

Comparing the upper with the corresponding lower panel of figure 1 shows that the probability  $\Gamma_{\varphi}(\mathbf{p}_1, \mathbf{p}_2)$  to find an electron pair in an accessible phase space island strongly changes from half-cycle to half-cycle. For example, in figure 1(a) and (c)  $\Gamma_{\varphi}(\mathbf{p}_1, \mathbf{p}_2)$  is practically zero in the two left most islands since the ionization rate  $R(t')$  is vanishingly small in these half-cycles. A similar situation is found for all other CE phase settings. In any case, at most two successive half-cycles contribute non-negligibly to NSDI. As will be seen below the complete calculation shows that for specific CE phase settings essentially only one half-cycle of the 4-cycle pulse is substantially giving rise to NSDI. For all other half-cycles the interplay of accessible final state phase space and the rate of ionization  $R(t')$  for the recolliding electron suppresses NSDI.

The electron sum-momentum distribution projected on the direction of the electric field of the light pulse is given by

$$\Gamma_{\varphi, \text{sum}, \parallel}(P_{\parallel}) = \int dp_{1,\parallel} \int d^2\mathbf{p}_{1,\perp} \int d^2\mathbf{p}_{2,\perp} \Gamma_{\varphi}(p_{1,\parallel}, \mathbf{p}_{1,\perp}, P_{\parallel} - p_{1,\parallel}, \mathbf{p}_{2,\perp}).$$

For the contact interaction used in our model the momentum integrations can be done analytically to give

$$\Gamma_{\varphi, \text{sum}, \parallel}(P_{\parallel}) \propto \int dt' R(t') \left\{ E_{\text{kin}}(t'') - I_p^+ - \frac{1}{4} [P_{\parallel} + 2A(t'')]^2 \right\}^{3/2} \quad (7)$$

with only the time integration left over all times  $t'$  with

$$E_{\text{kin}}(t'') - I_p^+ - \frac{1}{4} [P_{\parallel} + 2A(t'')]^2 \geq 0. \quad (8)$$

The factor which multiplies  $R(t')$  in the integrand is a measure of the volume of the accessible phase space for the momentum components which are integrated over. This electron sum-momentum distribution is equivalent to the corresponding momentum distribution of the doubly charged ion (here  $\text{Ar}^{++}$ ) which is formed in the ionization process. Conservation of the momentum of the atom during ionization gives rise to this correspondence. In the remaining part of the text we will always refer to the ion momentum distribution.  $\Gamma_{\varphi, \text{sum}, \parallel}(P_{\parallel})$  is shown in figure 2 for several

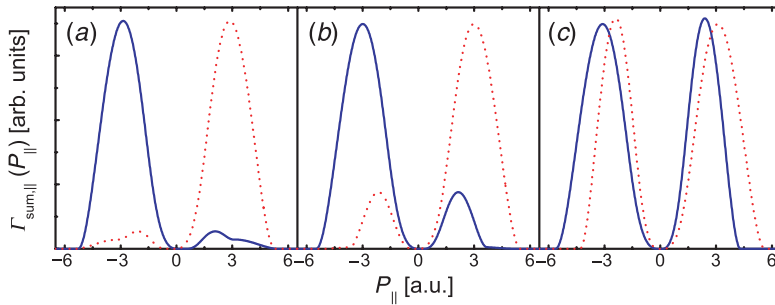


Figure 2. Numerical simulation of the momentum distribution of the doubly charged ions formed by NSDI in a few-cycle pulse at different CE phase settings  $\varphi$  (full line) and  $\varphi + \pi$  (dotted line): (a)  $\varphi = -0.3\pi$ , (b)  $\varphi = -0.1\pi$  and (c)  $\varphi = 0.15\pi$ . A 4-cycle laser pulse is used in the calculation. The parameters are the same as in figure 1. (The colour version of this figure is included in the online version of the journal.)

settings of the CE phase comprising those in figure 1. All parameters are the same as in figure 1. In each panel  $\Gamma_{\varphi, \text{sum}, ||}(P_{||})$  is plotted for a specific value of  $\varphi$  (full line) and for  $\varphi + \pi$  (dashed line). The corresponding ion momentum distributions are mirror images of each other with respect to reflection at  $P_{||} = 0$ . This is obvious from equation (7) since replacing  $\varphi$  by  $\varphi + \pi$  simply reverses the sign of the vector potential  $\mathbf{A}(t)$ . More generally,

$$\Gamma_{\varphi+\pi}(\mathbf{p}_1, \mathbf{p}_2) = \Gamma_{\varphi}(-\mathbf{p}_1, -\mathbf{p}_2).$$

The  $\text{Ar}^{++}$  ion momentum distribution shows a strong asymmetry for almost every setting of the CE phase. It is most pronounced for  $\varphi = -0.3\pi, 0.7\pi$  (figure 2(a)). Only a small ion emission probability is found for  $P_{||} < 0$  for  $\varphi = -0.3\pi$  and for  $P_{||} > 0$  at  $\varphi = 0.7\pi$ , respectively. This means, only one optical cycle of the 4-cycle pulse efficiently contributes to NSDI. Inspection of figure 1(a) and (c) (lower panel) shows that for these CE phase settings NSDI into the rightmost accessible phase space islands is suppressed despite the fact that the rate of electric field ionization  $R(t')$  for the recolliding electron reaches a maximum in the corresponding optical cycle (upper panel of figure 1(a) and (c)). The phase space volume which multiplies  $R(t')$  in equation (7) is responsible for suppression of NSDI in this half-cycle.

There are only two settings of the phase where the asymmetry in the ion momentum distribution is minimized. For the model calculation this is at  $\varphi = 0.15\pi$  and  $\varphi = 1.15\pi$  (figure 2(c)). But, even in these cases the momentum distribution is not really symmetric with respect to reflection at  $P_{||} = 0$ . The distribution maxima for negative and positive  $P_{||}$ , respectively, appear at slightly different positions and their widths are clearly different. A close interplay of the field ionization rate  $R(t')$  and the phase space volume in equation (7) is necessary to create the near symmetry of the ion momentum distribution since  $R(t')$  alone would give rise to preferred double ionization in one half-cycle only (see figure 1(b)). The positions and widths of the two classically accessible phase space islands which contribute to NSDI are mainly responsible for the positions and widths of the two maxima in the ion momentum distribution for  $\varphi = 0.15\pi, 1.15\pi$ .

The model shows that the final state momentum distribution after NSDI with few-cycle laser pulses depends critically on the cycle-dependent field ionization rate  $R(t')$  for the recolliding electron. Of equal importance is the volume of the classically accessible final phase space which is fixed by  $E_{\text{kin}}(t'') - I_p^+$  and its strong cycle dependence together with the cycle dependence of the time intervals where recollision may happen. In the model these three points work together to create the high sensitivity of the ion momentum distribution, and therefore of the whole electron momentum correlation, on the CE phase.

### 3. Experimental set-up

Measurement of the electron sum-momentum is based on cold target recoil ion momentum spectroscopy (COLTRIMS) [36] by measuring the momentum of the doubly charged ion emerging from NSDI. Our specific experimental set-up has been described in several recent publications (see for example [14, 20, 40]). A low-density ( $\approx 10^8$  atoms  $\text{cm}^{-3}$ ) supersonic argon atomic beam is hit by a laser beam at its focal spot. Both beams cross at right angles. The supersonic expansion and a high beam collimation precisely fix the momentum of the Ar atoms with only a small momentum spread. A weak electric field ( $1\text{--}7$  V  $\text{cm}^{-1}$ ) extracts the ions emerging from the interaction of the laser light with the Ar atoms. After passage of a drift tube they are recorded by a microchannel plate detector. The initial momenta they obtained by photoionization are determined from the measured time-of-flight and the position where they hit the detector. The extraction electric field brings about a solid angle of ion detection which amounts to  $4\pi$ .

Laser pulses are obtained from a commercial femtosecond oscillator and amplifier (Femtolasers GmbH) followed by a hollow fibre pulse compressor. This set-up generates  $500\ \mu\text{J}$  pulses with  $\approx 5$  fs pulse width at a centre wavelength of 760 nm. The CE phase is stabilized using a three-stage servo loop. The first and second stages stabilize the phase of the oscillator and amplifier, respectively [5]. Both employ the self-referencing scheme known from optical frequency metrology [3]. Long-term phase stability—the measurements required hours of data acquisition—is accomplished with the stereo-ATI method [6, 41]. Here spectra of high-energy (ATI) photoelectrons emitted in opposite directions along the light beam polarization axis are measured. A characteristic CE phase dependent left–right asymmetry between the two directions of emission allows one to determine the phase  $\varphi$ . Besides its use as a phasemeter, the stereo-ATI helps monitoring the laser performance and allows one to compensate long term phase drifts.

The whole experimental set-up is sketched in figure 3. A small fraction of the laser radiation is sent to the stereo-ATI apparatus by use of a beam splitter. Precise adjustment of the amount of glass (W2) in the beam path corrects for the difference in optical path lengths to the stereo-ATI and to the COLTRIMS apparatus. This ensures short pulses in both experiments simultaneously. Control of W2, however, does not imply identical values of  $\varphi$  in both experiments. In fact, the offset  $\Delta\varphi = \varphi_{\text{ATI}} - \varphi_{\text{COLTRIMS}}$  as well as  $\varphi_{\text{COLTRIMS}}$  itself are unknown during the experiment. However, what matters is a constant  $\Delta\varphi$ . In order to actively control the CE

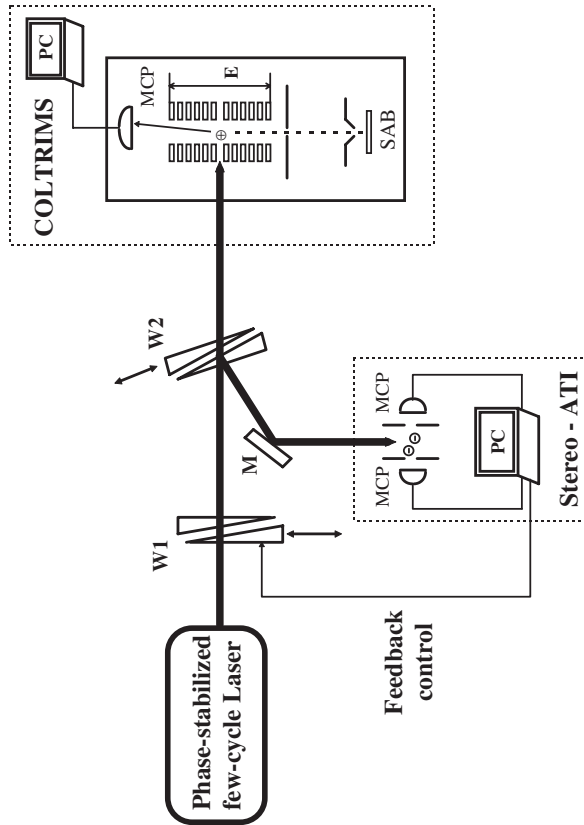


Figure 3. Schematic view of the experimental set-up. W1, W2: two pairs of glass wedges; MCP: position sensitive microchannel plate detector; M: mirror; E: extraction electric field; SAB: supersonic atomic beam.

phase, the pair of glass wedges (W1) in the common beam path is automatically adjusted by a correction signal which is supplied by the ATI phasemeter. Hence, during the whole measurement the CE phase  $\varphi_{\text{ATI}}$  is measured and kept at a fixed value. In order to scan different values of  $\varphi_{\text{COLTRIMS}}$ , the amount of glass of W2 and therefore  $\Delta\varphi$  is changed by known amounts. For example, an addition of  $26\ \mu\text{m}$  of fused silica into the beam path changes  $\varphi$  by  $\pi$ .

#### 4. The experimental results

In the experiment we investigated NSDI of argon. Figure 4 shows the measured  $\text{Ar}^{++}$  ion momentum distributions for different CE phase settings. The 3D distribution  $f(\mathbf{P}_{\perp}, P_{\parallel})$  is projected on the laser polarization direction, i.e. the distribution  $f_{\parallel}(P_{\parallel}) = \int d^2\mathbf{P}_{\perp} f(\mathbf{P}_{\perp}, P_{\parallel})$  is shown in the figure. The laser pulse width was fixed to  $\approx 5\ \text{fs}$  and the light intensity to  $\approx 350\ \text{TW cm}^{-2}$ . Qualitatively similar to our model results, we find indeed a prominent asymmetric pattern in the momentum

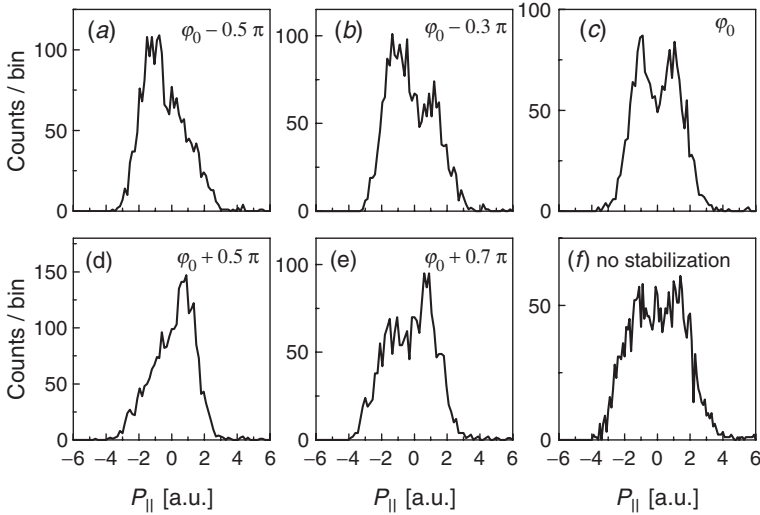


Figure 4. Experimental momentum distribution of  $\text{Ar}^{2+}$  ions from NSDI of Ar at different CE phase settings  $\varphi$ . The laser pulse parameters are  $\approx 5$  fs pulse width and  $\approx 350 \text{ TW cm}^{-2}$  peak light intensity. The distributions shown are integrated over the Cartesian momentum components perpendicular to the light beam polarization axis.  $\varphi_0$ , shown on the panels, is determined from comparison with a theoretical model to be  $0.15\pi \pm 0.1\pi$ . The spectrum in panel (f) was taken with unstabilized phase at otherwise unchanged experimental parameters.

distributions which changes significantly with the setting of the CE phase. A nearly symmetric distribution is found only at one specific setting of the phase ( $\varphi = \varphi_0$ ). As expected, switching off the phase stabilization of the laser gives rise to a symmetric ion momentum distribution (figure 4(f)). The symmetric spectrum at the phase setting  $\varphi = \varphi_0$  and the spectrum at random phase clearly point to Ar being double ionized non-sequentially even in the few optical cycle limit. They closely resemble ‘long pulse spectra’ at light intensities where Ar double ionization proceeds predominantly non-sequentially [13, 14, 20]. Moreover, sequential double ionization with both electrons leaving the atom uncorrelated should show a similar phase dependence as single ionization. There integrated phase effects have been found to be of the order of only 10% [6]. This is much less than we find here for double ionization. There are several points to be noted in figure 4. (i) The fixed phase symmetric distribution at  $\varphi = \varphi_0$  is slightly narrower than the distribution measured with free-running phase at the same light intensity. (ii) The minimum in the  $\text{Ar}^{++}$  yield at  $P_{\parallel} = 0$  is more pronounced in the fixed phase spectrum. (iii) A phase change of  $\pi$  transforms the momentum distribution into its mirror image after reflection at  $P_{\parallel} = 0$  (compare figure 4(a) and (d), (b) and (e)). This last point is obvious in view of the discussion above in connection with our model.

In the experimental spectra one unknown quantity remains, the actual value of the CE phase which is fixed by determining  $\varphi_0$ . It is not possible to extract  $\varphi_0$  from the experimental data alone. To fix it, based on the NSDI data, one should resort to an exact calculation of the ion momentum distribution. Since this is not feasible we

use our model to determine  $\varphi_0$ . The starting point is the nearly symmetric distribution. Comparing figure 4(c) with the calculated spectra (figure 2) one gets  $\varphi_0 = 0.15\pi$  or  $\varphi_0 = 1.15\pi$ . The relative change of the CE phase necessary to get the asymmetric spectra correct (figure 4(a), (b), (d) and (e)) then finally fixes  $\varphi_0$  to be  $0.15\pi$ . From the comparison of the calculated and measured spectra an uncertainty in the phase of  $\pm 0.1\pi$  remains. The phase convention used here is fixed by the choice of the vector potential in equation (1). One has to bear in mind that the way we determined the CE phase may depend on the model we use to calculate the momentum distributions. A first consistency check would be to compare with the CE phase derived from above-threshold single ionization using the stereo-ATI technique [6]. However, to have a reliable comparison both measurements have to be done in the same experimental set-up under identical conditions.

Overall we find the agreement between our simple classical model and the experimental results encouraging, even if a closer comparison reveals several discrepancies. (i) The calculated yield of  $\text{Ar}^{++}$  ions with momentum  $P_{\parallel} \approx 0$  is always close to zero whereas the yield found in the experiment is significantly different from 0. (ii) At  $\varphi = -0.3\pi$  and at  $\varphi = 0.7\pi$  nearly all ions are found with either  $P_{\parallel} > 0$  or  $P_{\parallel} < 0$  in the calculation. The experiment shows distributions with a clear ‘hanging shoulder’ at these phases but a significant amount of ions is always found with a momentum opposite to that of the main maximum. (iii) The separation of the maxima in the experiment is smaller than that found in the calculated spectra.

Concerning points (i) and (ii) it is important to note that in the recollision on the ion core besides impact ionization a second significant NSDI channel exists for Ar, namely impact excitation of  $\text{Ar}^+$  into bound excited states. Subsequently, the excited electron is electric field ionized in one of the following half-cycles of the light pulse [16, 30, 31]. This double ionization mechanism allows the formation of photoelectron pairs with similar momenta emitted in opposite directions, thus giving rise to  $\text{Ar}^{++}$  ions with  $P_{\parallel} \approx 0$ . In the classical model this channel has not been taken into account. For the phase settings where the most pronounced asymmetric ion momentum distributions are found (figure 4(a) and (d)) approximately three significant half-cycles in the trailing part of the pulse are available to accomplish ionization of the excited  $\text{Ar}^+$  states. This can be seen by inspection of figure 1 (a) and (c). In  $\text{Ar}^+$  the lowest-lying excited states which may be populated efficiently in the collision have the electron configuration  $3s^23p^43d$  [16]. The ionization potential of an electron in one of these states is less than 11.2 eV. Using electric field ionization to describe the ionization of the excited states it can be easily seen that the amplitudes of the trailing half-cycles in the pulse suffice for above barrier ionization of all of the excited states. This means, even in a few-cycle pulse this NSDI channel is not efficiently suppressed. To learn more about the influence of this channel it will be necessary in the future to determine the full final state electron momentum correlation. The symmetry properties of the momentum correlation may give insight into the time it takes to remove the second electron from the excited state.

The differing widths we found in the calculated and measured ion momentum distributions may have its origin in the model we use for the analysis. Specifically, the three-body contact interaction taken to describe the inelastic collision is known to

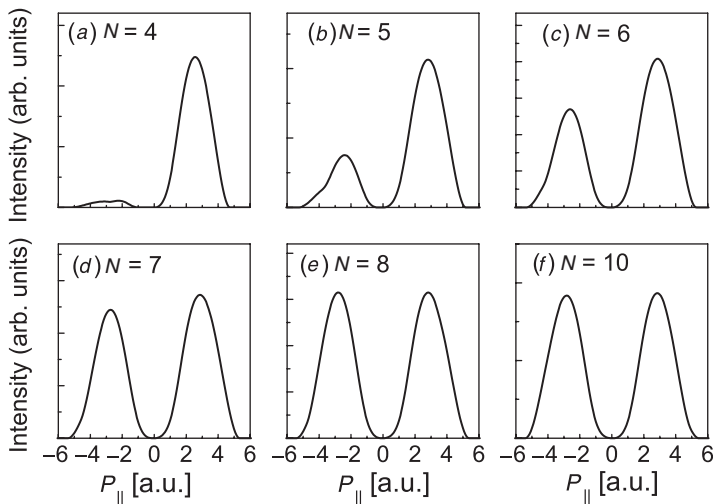


Figure 5. Model  $\text{Ar}^{++}$  ion momentum distributions for  $N$ -cycle pulses with the cycle number varying between  $N=4$  and  $N=10$ . The CE phase setting is always the same ( $\varphi = -0.3\pi$ ). The light intensity was chosen to be  $350 \text{ TW cm}^{-2}$ .

result in a separation of the maxima in the ion momentum distribution usually somewhat larger than observed experimentally [30].

The effect of the CE phase on the final state ion momentum distribution is expected to depend sensitively on the width of the laser pulse. For the impact ionization channel the model can give insight into this dependence. It is shown in figure 5 as a function of the number  $N$  of cycles of the laser pulse up to  $N = 10$ . The phase was set to  $\varphi = -0.3\pi$  where for the 4-cycle pulse the most pronounced asymmetry in the ion momentum distribution was found. The light intensity was again set to  $350 \text{ TW cm}^{-2}$  and the ionization potentials are those for Ar and  $\text{Ar}^+$ . It can be seen that already in an 8-cycle pulse the sensitivity of the ion momentum distribution on the CE phase disappears. It becomes symmetric with respect to reflection at  $P_{||} = 0$  to a high degree of accuracy. Varying  $\varphi$  does not change this symmetry. Eight cycles in our model correspond to a width of the pulse intensity distribution of only  $\text{FWHM} \approx 8 \text{ fs}$ .

## 5. Conclusions

In conclusion, our experimental study shows that the ion momentum distribution following NSDI in a few-cycle laser pulse reacts very sensitively to the CE phase  $\varphi$ . Consequently, via control over  $\varphi$  it is possible to direct non-sequential double ionization dynamics. The analysis of the experimental data through a classical model calculation reveals that the influence of the optical phase enters via the cycle-dependent electric field ionization rate, the electron recollision time and the accessible phase space for inelastic collisions. It also shows that the combination of

these effects allows one to look into single-cycle dynamics already for few-cycle pulses, since, depending on the phase, only one or at most two optical half-cycles effectively contribute to NSDI. The model shows that the influence of the CE phase is only present in the limit of very few cycles. It disappears already for a light pulse consisting of 8 optical cycles. Being able to steer NSDI by controlling the recolliding electrons via the CE phase goes well beyond NSDI itself. As proposed recently [32], recolliding electrons may be used as an efficient probe for the attosecond time domain, comparable to the presently used attosecond XUV pulses [33]. Our work now demonstrates that it is possible to control electrons coherently in space and in time via controlling the CE phase.

## Acknowledgments

We gratefully acknowledge support by the Deutsche Forschungsgemeinschaft (DFG) and fruitful discussions with W. Becker and C. Figueira de Morisson Faria. E. Goulielmakis and K. O’Keeffe have been supported by the Austrian Science Funds (Grant No. F016, P14447, P15382 and Z63). G.G. Paulus acknowledges support from The Welch Foundation.

## References

- [1] M. Nisoli, S. de Silvestri, O. Svelto, *et al.*, *Opt. Lett.* **22** 522 (1997); G. Steinmeyer, D.H. Sutter, L. Gallmann, *et al.*, *Science* **286** 1507 (1999).
- [2] T. Brabec and F. Krausz, *Rev. Mod. Phys.* **72** 545 (2000).
- [3] J. Reichert, R. Holzwarth, Th. Udem, *et al.*, *Opt. Commun.* **172** 59 (1999); H.R. Telle, G. Steinmeyer, A.E. Dunlop, *et al.*, *Appl. Phys. B* **69** 327 (1999).
- [4] D.J. Jones, S.A. Diddams, J.K. Ranka, *et al.*, *Science* **288** 635 (2000); A. Apolonski, A. Poppe, G. Tempea, *et al.*, *Phys. Rev. Lett.* **85** 740 (2000).
- [5] A. Baltuška, Th. Udem, M. Uiberacker, *et al.*, *Nature* **421** 611 (2003).
- [6] G.G. Paulus, F. Lindner, H. Walther, *et al.*, *Phys. Rev. Lett.* **91** 253004 (2003).
- [7] A. L’Huillier, L.A. Lompre, G. Mainfray, *et al.*, *Phys. Rev. A* **27** 2503 (1983).
- [8] D.N. Fittinghoff, P.R. Bolton, B. Chang, *et al.*, *Phys. Rev. Lett.* **69** 2642 (1992).
- [9] B. Walker, B. Sheehy, L.F. DiMauro, *et al.*, *Phys. Rev. Lett.* **73** 1227 (1994).
- [10] D.N. Fittinghoff, P.R. Bolton, B. Chang, *et al.*, *Phys. Rev. A* **49** 2174 (1994).
- [11] S. Augst, A. Talebpour, S.L. Chin, *et al.*, *Phys. Rev. A* **52** R917 (1995).
- [12] P. Dietrich, N.H. Burnett, M. Ivanov, *et al.*, *Phys. Rev. A* **50** R3585 (1994).
- [13] Th. Weber, M. Weckenbrock, A. Staudte, *et al.*, *Phys. Rev. Lett.* **84** 443 (2000).
- [14] R. Moshhammer, B. Feuerstein, W. Schmitt, *et al.*, *Phys. Rev. Lett.* **84** 447 (2000).
- [15] Th. Weber, H. Giessen, M. Weckenbrock, *et al.*, *Nature* **405** 658 (2000).
- [16] B. Feuerstein, R. Moshhammer, D. Fischer, *et al.*, *Phys. Rev. Lett.* **87** 043003 (2001).
- [17] R. Moshhammer, B. Feuerstein, J. Crespo Lopez-Urrutia, *et al.*, *Phys. Rev. A* **65** 035401 (2002).
- [18] R. Moshhammer, J. Ullrich, B. Feuerstein, *et al.*, *J. Phys. B: At. Molec. Opt. Phys.* **36** L113 (2003).
- [19] M. Weckenbrock, A. Becker, A. Staudte, *et al.*, *Phys. Rev. Lett.* **91** 123004 (2003).
- [20] E. Eremina, X. Liu, H. Rottke, *et al.*, *J. Phys. B* **36** 3269 (2003).
- [21] M. Weckenbrock, D. Zeidler, A. Staudte, *et al.*, *Phys. Rev. Lett.* **92** 213002 (2004).

- [22] V.L.B. de Jesus, A. Rudenko, B. Feuerstein, *et al.*, J. Electron. Spectrosc. Rel. Phenom. **141** 127 (2004).
- [23] B. Witzel, N.A. Papadogiannis and D. Charalambidis, Phys. Rev. Lett. **85** 2268 (2000).
- [24] R. Lafon, J.L. Chaloupka, B. Sheehy, *et al.*, Phys. Rev. Lett. **86** 2762 (2001).
- [25] E.R. Peterson and P.H. Bucksbaum, Phys. Rev. A **64** 053405 (2001).
- [26] J.L. Chaloupka, J. Rudati, R. Lafon, *et al.*, Phys. Rev. Lett. **90** 033002 (2003).
- [27] P.B. Corkum, Phys. Rev. Lett. **71** 1994 (1993).
- [28] M. Ferray, A. L'Huillier, X.F. Li, *et al.*, J. Phys. B: At. Molec. Opt. Phys. **21** L31 (1988).
- [29] G.G. Paulus, W. Nicklich, H. Xu, *et al.*, Phys. Rev. Lett. **72** 2851 (1994).
- [30] R. Kopold, W. Becker, H. Rottke, *et al.*, Phys. Rev. Lett. **85** 3781 (2000).
- [31] V.L.B. de Jesus, B. Feuerstein, K. Zrost, *et al.*, J. Phys. B: At. Molec. Opt. Phys. **37** L167 (2004).
- [32] H. Niikura, F. Légaré, R. Hasbani, *et al.*, Nature **417** 917 (2002).
- [33] R. Kienberger, E. Goulielmakis, M. Uiberacker, *et al.*, Nature **427** 817 (2004).
- [34] X. Liu and C. Figueira de Morisson Faria, Phys. Rev. Lett. **92** 133006 (2004).
- [35] X. Liu, H. Rottke, E. Eremina, *et al.*, Phys. Rev. Lett. **93** 263001 (2004).
- [36] J. Ullrich, R. Moshhammer, A. Dorn, *et al.*, Rep. Prog. Phys. **66** 1463 (2003).
- [37] M.V. Ammosov, N.B. Delone and V.P. Krainov, Zh. Eksp. Teor. Fiz. **91** 2008 (1986) [Sov. Phys. JETP **64** 1191 (1986)].
- [38] C. Figueira de Morisson Faria, X. Liu, W. Becker, *et al.*, Phys. Rev. A **69** 021402(R) (2004); C. Figueira de Morisson Faria, H. Schomerus, X. Liu, *et al.*, Phys. Rev. A **69** 043405 (2005).
- [39] L.V. Keldysh, Zh. Eksp. Teor. Fiz. **47** 1945 (1964) [Sov. Phys. JETP **20** 1307 (1965)].
- [40] E. Eremina, X. Liu, H. Rottke, *et al.*, Phys. Rev. Lett. **92** 173001 (2004).
- [41] G.G. Paulus, F. Grasbon, H. Walther, *et al.*, Nature **414** 182 (2001).